Magnetic and magnetothermal properties and the magnetic phase diagram of high purity single crystalline terbium along the easy magnetization direction

2014 J. Phys.: Condens. Matter 26 066001

(http://iopscience.iop.org/0953-8984/26/6/066001)

IOP Publishing Journal of Physics: Condensed Matter
J. Phys.: Condens. Matter **26** (2014) 066001 (7pp) doi:10.1088/0953-8984/26/6/066001

Magnetic and magnetothermal properties and the magnetic phase diagram of high purity single crystalline terbium along the easy magnetization direction

V I Zverev[1,2], A M Tishin[1,2], A S Chernyshov[3], Ya Mudryk[4], K A Gschneidner Jr[4,5] and V K Pecharsky[4,5]

[1] Faculty of Physics, M V Lomonosov Moscow State University, 119991, Moscow, Russia
[2] Advanced Magnetic Technologies and Consulting LLC, 142190, Troitsk, Russia
[3] Western Digital, Advanced Media Development 1710 Automation Pkwy, San Jose, CA 95131, USA
[4] The Ames Laboratory, US Department of Energy, Iowa State University, Ames, IA 50011-3020, USA
[5] Department of Materials Science and Engineering, Iowa State University, Ames, IA 50011-2300, USA

E-mail: vi.zverev@physics.msu.ru

Received 14 September 2013, revised 20 November 2013
Accepted for publication 9 December 2013
Published 21 January 2014

Abstract
The magnetic and magnetothermal properties of a high purity terbium single crystal have been re-investigated from 1.5 to 350 K in magnetic fields ranging from 0 to 75 kOe using magnetization, ac magnetic susceptibility and heat capacity measurements. The magnetic phase diagram has been refined by establishing a region of the fan-like phase broader than reported in the past, by locating a tricritical point at 226 K, and by a more accurate definition of the critical fields and temperatures associated with the magnetic phases observed in Tb.

Keywords: magnetic materials, rare-earth metals, single crystalline terbium, phase diagram, magnetic transitions

(Some figures may appear in colour only in the online journal)

1. Introduction

The rare-earth metal Tb has the second largest spin moment among lanthanide metals and its total magnetic moment, 9 μ_B, is next to Dy and Ho. Tb crystallizes in the hexagonal close packed (hcp) structure [1]. Magnetization data of polycrystalline terbium over the temperature range from 4 to 375 K in magnetic fields ranging from 50 Oe to 18 kOe were first reported by Thoburn *et al* [2]. Measurements in weak magnetic fields from 50 to 800 Oe indicated a paramagnetic (PM)–antiferromagnetic (AFM) order–disorder transition at ~230 K. It was also suggested that terbium is a weak antiferromagnet (of an unknown type) between ~218 and 230 K. The AFM state vanishes in magnetic fields exceeding 200 Oe, being replaced by the ferromagnetic (FM) state. Below 218 K, Tb was reported to be a ferromagnet. A few years later, magnetization measurements along all crystallographic directions were repeated on single crystalline Tb by Hegland *et al* [3]. The results generally agreed with those of the polycrystalline sample, with the exception of the Curie and Néel temperatures, that were reported as 221 K and 229 K, respectively.

The magnetic structure of terbium was investigated by neutron scattering [4]. Koehler *et al* reported that in the narrow AFM region the magnetic structure of Tb is helical or spiral. The interlayer turn angle varies from 20.5° per layer at the Néel point (229 K) to 18.5° per layer at the AFM–FM transition (218 K). In the ferromagnetic state the moments (~9.0 μ_B per Tb atom) were reported to be in the basal plane. Similar to dysprosium [5], the AFM–FM transition in terbium is a magnetostructural transformation (MST) observed in the vicinity of the Curie point in both zero and non-zero external magnetic fields. According to x-ray diffraction measurements

by Darnell [6], the crystallographic symmetry is reduced from hexagonal to orthorhombic at 218 K.

Dietrich *et al* [7] have reported that the transition between the FM and spiral (helical) structure is of the first order; they also determined the Néel temperature to be ∼226 K and have shown that in the close vicinity of this temperature the turn angle per layer for the helix varies from 20.7° at 226 K to 16.5° at 216 K, which is in good agreement with previous data [4].

In addition to the well known magnetic phases observed in Tb by various experimental techniques, the question of whether the fan phase exists is still under debate. The theoretical description of the fan structure is given in [1] as a structure in which the moments make an angle θ with the field direction. The opening angle of the fan thus goes continuously to zero at the second-order transition to the ferromagnetic phase. In the antiferromagnetic phase, the application of low magnetic fields in the basal plane of the helical structure should cause a distortion of the helix. According to Nagamiya and Kitano [8], the moments antiparallel to the field rotate when a critical field is exceeded, forming a fan state. The suggestion that the fan phase is possible in Tb was made after a transition from the fan phase to the ferromagnetic state was first indicated by the minimum in the field dependence of the elastic modulus constant c_{33} in Dy [9]. Later, the existence of this phase in Dy was supported by other experimental methods [10, 11]. Analogous to Dy, the anomaly of elastic modulus (the minimum of c_{33} in fields higher than 3.5 kOe in the temperature range 214–218 K) measured by Jiles *et al* [12] has been considered a signature of the fan structure in Tb. However, the authors also note that, instead of a fan, a distorted helical structure in which large ferromagnetic regions had grown from domain walls aligned parallel to the field direction is also possible. Because of rather contradictory evidence, the fan phase was not included on the phase diagram of Tb in [12].

The elastic modulus of terbium has been re-investigated as a function of temperature between 200 and 230 K as a function of magnetic field applied along the easy magnetization direction [13]. Based on the observed anomalies in the elastic constants, a magnetic phase diagram was constructed with the Curie temperature at 219.5 K and the Néel temperature at ∼230 K. Since the values of the critical fields reported by the authors differed by as much as a factor of two from those of previously published results, it was concluded that sample purity is of crucial importance in studying the intrinsic behavior of the antiferromagnetic phase of terbium.

The existence of the fan phase in dysprosium and related rare-earth metals was shown theoretically by Bagguley *et al* [14]. The authors consider the fan as the evolution of a spiral structure with increasing external magnetic field, but at the same time there may be multiple factors (including sample purity, that leads to different domain wall configurations) which can influence the behavior of the transition from the FM or helical state, and this is why the existence or the absence of the fan phase should be determined in each case. To the best of our knowledge, this phase has only been observed experimentally by measuring the elastic and acoustic properties in magnetic fields [15] (at the same time, the critical field values determined in the paper have not been corrected for demagnetization); none of the other techniques employed have revealed the fan phase in Tb. For example, measurements of the magnetocaloric effect (MCE) of a Tb single crystal in weak magnetic fields <0.1 T in the temperature interval 220–230 K indicated the existence of a tricritical point at 228.5 K, and even allowed the authors [16] to construct the magnetic phase diagram in the basal plane, but it was impossible to determine the boundaries of the fan phase from MCE measurements. Thus, the only phase diagram of Tb which includes the fan phase was proposed by Kataev *et al* [17]. Combining the data from elastic, magnetic and magnetocaloric measurements, the authors constructed the phase diagram, which mainly repeats the previous ones and also includes the region of the fan phase in the 222–228 K interval from 100 to 300 Oe. Outside this region the fan phase is suppressed.

Jennings *et al* [18] measured the heat capacity of terbium in the temperature range from 15 to 350 K. A lambda-type anomaly was observed at 227.7 K. There was also another anomaly near 220 K. The magnetic contribution to the heat capacity, C_M, was estimated and agreed well with the known magnetization and electrical resistivity data [19].

In the past, the magnetic and thermal properties of single crystal Tb were studied using different quality samples, in most cases on samples of unknown and, often, low purity. There is surprisingly little (e.g. in comparison with other rare-earth metals Ho and Dy) information about the magnetic phases existing in Tb, especially about the fan phase. In addition, there also has been a large spread of reported values of the critical fields and temperatures, which is probably associated with the different experimental techniques used and different purities of the samples. A thorough investigation of the magnetic and thermal properties of high purity single crystals of Tb is of fundamental importance, because magnetic phase transitions may be strongly affected if the total concentration of impurities exceeds a few hundred ppm by weight [20] (we note that concentrations of interstitial impurities are high, but generally their levels are not quoted in commercially available lanthanides). In this paper we report measurements carried out using high purity Tb crystals with the magnetic field applied parallel to the *b* (in-plane) direction using dc-magnetization, ac magnetic susceptibility, and heat capacity measurements as a function of temperature and applied magnetic field. The terbium magnetic phase diagram generated from this investigation is compared with previously known data [21–23].

2. Experimental details

The single crystals of Tb were prepared by the Materials Preparation Center at the Ames Laboratory[6]. The major impurities in the polycrystalline metal used to grow the single crystal using a strain-anneal process [24] were as

[6] Materials Preparation Center, Ames Laboratory of US Department of Energy, Ames, IA, (www.mpc.ameslab.gov).

follows (in ppm at.): O, 1900; C, 1100; N, 180; F, 40; Cl, 33; Fe, 20; Al, 5; Cr, 4.4; Cu, 2.3; Si, 2; thus the starting material was 99.67 at.% (99.993 wt%) pure. The material has a residual resistivity ratio of 160. Crystallographic directions were determined using the back reflection Laue technique. The combined accuracy of the alignment of the crystallographic axes with the direction of the magnetic-field vector was ±5°. The sample for the dc-magnetization and ac magnetic susceptibility measurements was cut in the shape of a parallelepiped, $0.96 \times 2.85 \times 0.56$ mm^3 (mass 9.8 mg), by using the spark-eroding technique from a large grain. The longest axis of the parallelepiped was aligned parallel to the *b* crystallographic axis ([110] crystallographic direction) of Tb. The sample for the heat capacity measurements, also cut from a large grain of the same specimen, was a flat cylinder, 3 mm high, and 10 mm in diameter. The *b* crystallographic axis was perpendicular to the plane of the sample.

All isothermal magnetization measurements have been corrected for demagnetization [25]. The value of the demagnetization factor was 0.10. The dc-magnetization data (isothermal magnetic-field dependences and isofield temperature dependences) and the ac magnetic susceptibility were measured using a Quantum Design MPMS-XL7 magnetometer. Magnetic measurements were made in external magnetic fields varying from 0 to 70 kOe and over the temperature interval from 5 to 300 K. The rms (root mean square) amplitude of the ac magnetic field was 2.5 Oe, and the ac magnetic field working frequency was 125 Hz. The accuracy of the magnetic measurements is better than 1%.

The heat capacity in constant magnetic fields ranging from 0 to 75 kOe was measured between 1.5 and 350 K in a semiadiabatic heat pulse calorimeter, which has been described elsewhere [26]. The accuracy of the heat capacity data was better than ∼0.6% in the temperature interval from 20 to 350 K and better than ∼1% in the temperature range 4–20 K.

3. Magnetic properties

The isothermal dependences of the magnetization of the Tb single crystal measured from 5 to 212 K with the magnetic field applied parallel to the *b* axis are shown in figure 1.

The experimental results are in good agreement with the previous data [2, 3]. The magnetization is nearly saturated at 6 kOe. The saturation value of ∼9.02 μ_B (∼315 emu g^{-1}) at 5 K is in good agreement with previous experimental data [3] and the theoretical $gJ = 9$ μ_B [1]. In the given temperature interval, Tb is reported to be a simple ferromagnet and no metamagnetic features indicating field-induced phase transitions are expected or seen, even at fields much lower than the saturation fields.

Above 212 K but below 221 K (figure 2(a)), Tb exhibits no magnetic-field-induced transitions.

Further, no anomalies are seen in the isofield magnetic measurements of heat capacity (see below) and magnetic susceptibility (not shown) at temperatures below 221 K,

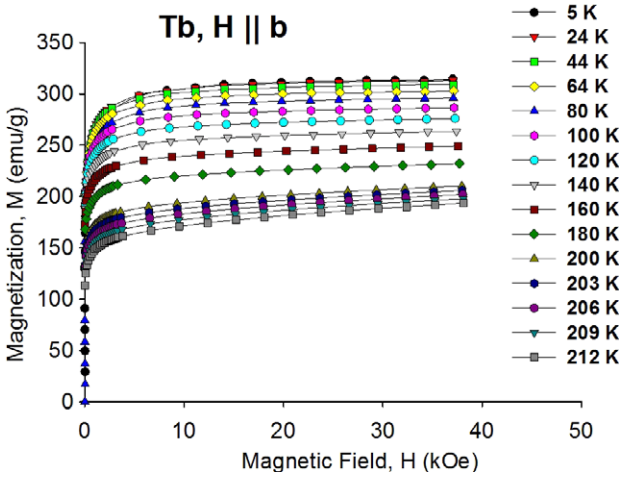

Figure 1. Isothermal magnetization of Tb measured between 5 and 212 K with the magnetic-field vector parallel to the *b* axis in magnetic fields from 0 to 40 kOe.

which leads to the conclusion that there are no field-induced transitions in Tb below 221 K, and it behaves as a typical ferromagnetic material.

It is common for rare-earth metals with helical ordering that the magnetization first nearly linearly increases with the magnetic field, and when the field exceeds some critical value an abrupt change in the magnetization is observed, after which it relatively quickly saturates below the Néel temperature. Thus, in Tb weak metamagnetic-like features in the magnetization corresponding to a magnetic-field-induced AFM–FM transformation are observed above 221 K. Only the low field parts of the magnetization curves are shown in figure 2(b) for clarity, since metamagnetic features are not noticeable at higher fields. In contrast with previous investigations, we collected $M(H)$ data including low fields, which was not done in the past due to large demagnetizing fields.

Oosthuizen *et al* [27] constructed the magnetic phase diagram based on $M(H)$ and $M(T)$ measurements. The values of the critical fields have been estimated from intersections of extrapolated linear parts of the magnetization curves, since the authors did not have reliable data in the low field region. As a result, the phase diagram represents only three phases, with the helix AFM phase between 221 and 228 K and in the field interval limited to 150 Oe. At the same time, the errors in determination of the critical fields were as large as one-third of the values themselves due to the interpolation procedure. By minimizing the demagnetization factor (i.e. having an elongated sample) we were able to measure magnetization values in the low field region. This may be not crucial for temperatures below 220 K, but becomes quite important at higher temperatures. Our results show that the helix AFM phase exists from 221 to 228 K and from ∼10 to ∼150 Oe. The critical field associated with the FM to helix AFM transition first increases from ∼10 Oe at 221 K to ∼150 Oe (the maximum value at 226 K) and then decreases to zero at the Néel point, 228 K (see figure 3), where the AFM phase is completely suppressed.

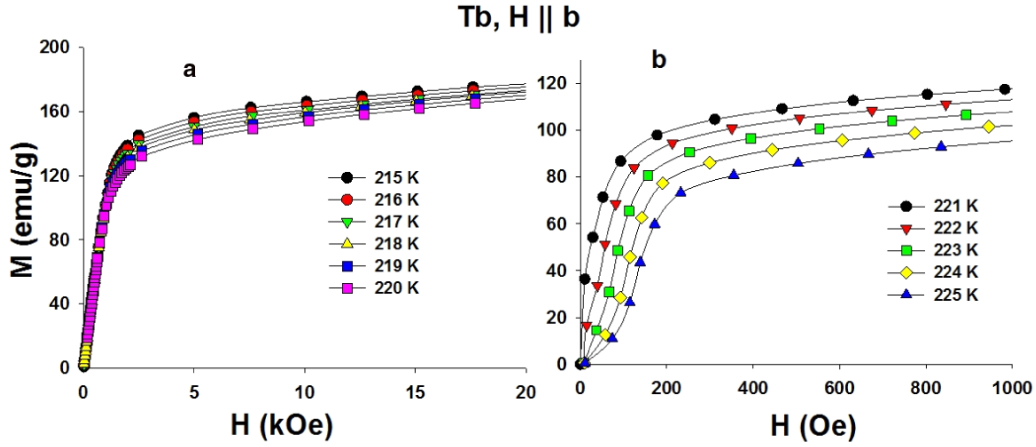

Figure 2. (a) Isothermal magnetization of Tb measured between 215 and 220 K with the magnetic-field vector parallel to the *b* axis in magnetic fields from 0 to 20 kOe. (b) Isothermal magnetization of Tb measured between 221 and 225 K with the magnetic-field vector parallel to the *b* axis in magnetic fields from 0 to 1 kOe. The data have been corrected for demagnetization.

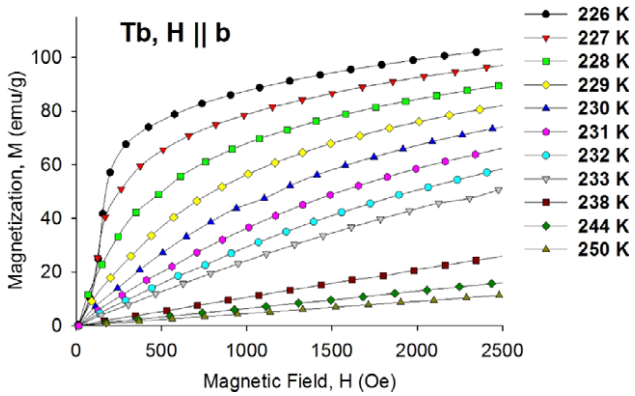

Figure 3. Isothermal magnetization of Tb measured between 226 and 250 K with the magnetic-field vector parallel to the *b* axis in magnetic fields from 0 to 2.5 kOe.

A step-like increase in the magnetization is clearly observed at 227 K, but at 228 K, which is the Néel temperature, it is reduced to a change of slope of the $M(H)$ function. At 229 K and higher temperatures there are no metamagnetic features in magnetization curves, as Tb adopts the paramagnetic state, and at temperatures higher than 244 K the behavior of the magnetization becomes nearly linear. The $M(H)$ curves measured just above the Néel temperature (229–239 K) are not straight lines in the low field region, which is associated with a continuous character of the second-order AFM–PM transition, and with spin fluctuations that persist well above the magnetic ordering temperature.

Thus the analysis of the $M(H)$ curves indicates that Tb is ferromagnetic up to 221 K, that from 221 to 228 K in fields of 0–150 Oe helical AFM structure is observed, and that above 228 K it is paramagnetic. Unlike the case in some of the previous studies, there is no evidence of a fan structure in our isothermal magnetic measurements. Greenough *et al* [28] argued that limited appearance of a linear region near the knee of the magnetization curves at $T_C < T < 222.8$ K indicates the existence of fan structure which is restricted by a narrow temperature interval just above the Curie temperature. Since the samples used in [28] were spherical in shape, internal field was strongly affected by demagnetization, and $M(H)$ data in the fields below 200 Oe were not presented. Further, the linear regions in the magnetization curves observed above the Curie temperature may have been associated with experimental errors because they did not account for the demagnetization factor. We also note that the residual resistivity ratio for the sample used in [28] was 120, indicating a high purity of the material. Thus, one can reasonably conclude that it is difficult, and even may be impossible, to prove the existence of the fan phase in Tb using only magnetic measurements.

The temperature dependence of the magnetization along the *b* axis measured at 50 and 100 Oe is shown in figures 4(a) and (b).

Peaks observed at 220 and 228 K at 50 Oe (inset, figure 4(a)) and at the same temperatures at 100 Oe correspond to the first-order FM–AFM and second-order AFM–PM magnetic phase transitions, respectively. The $M(T)$ data are in good agreement with the previously published results [3]. The AFM–PM transition shifts towards lower temperatures with increasing magnetic field, as is typical for antiferromagnets. For the 100 Oe data at temperatures below 221 K, the magnetization behavior of the zero-field-cooled (ZFC) sample (measurements on heating) is significantly different from the same measured during cooling in field (FC) (see figure 4(b)). Once the material forms domains below the ordering temperature, magnetic field higher than coercive field is required to align them. When the sample is cooled in low field from room temperature the domains align easily just below the Curie temperature (low coercive field), and when the sample is heated after being cooled in zero field the domains may become 'pinned' (high coercive field), resisting the alignment until warmed up. In figure 4(b) one can see that the coercive field is higher than 100 Oe up to the Curie temperature, where the ferromagnetic ordering is beginning to be replaced by the intermediate phase. There is a small temperature hysteresis for the Curie temperature (the first peak in the $M(T)$ dependence), which confirms the first-order character of the AFM–FM

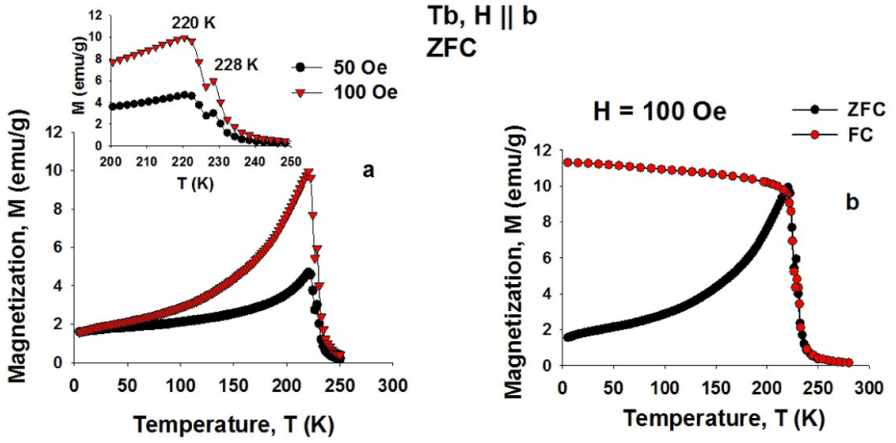

Figure 4. (a) Isofield magnetization of Tb measured during zero-field-cooled heating from 5 to 250 K with the 50 and 100 Oe magnetic field parallel to the *b* axis. The inset shows the expanded view of the region between 200 and 250 K. (b) Isofield magnetization with the 100 Oe magnetic field from 5 to 280 K measured during zero-field-cooled heating and field-heated cooling.

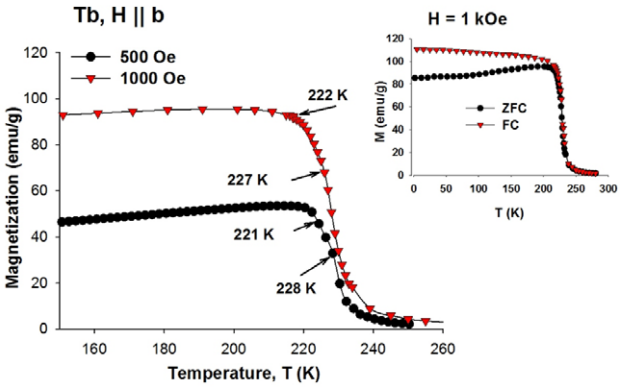

Figure 5. Isofield magnetization of Tb measured during zero-field-cooled heating from 150 to 260 K with the 500 and 1000 Oe magnetic fields parallel to the *b* axis. The inset shows isofield magnetization of Tb measured during zero-field-cooled heating and field-heated cooling from 5 to 280 K with the 1000 Oe magnetic field parallel to the *b* axis.

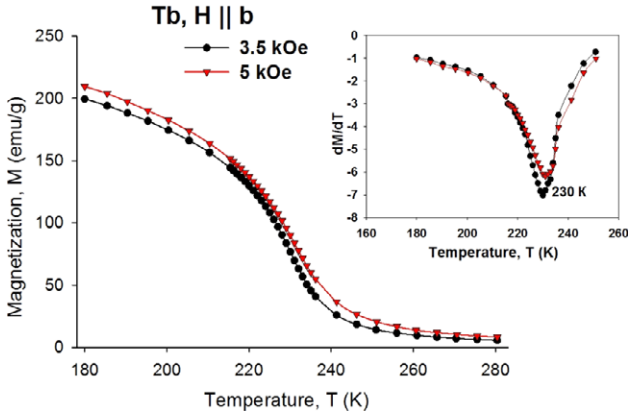

Figure 6. Isofield magnetization of Tb measured during zero-field-cooled heating from 180 to 280 K with 3.5 and 5 kOe magnetic fields parallel to the *b* axis. The inset shows the behavior of the $\mathrm{d}M/\mathrm{d}T$ dependences in the same temperature range.

transition. At the same time, no hysteresis is observed for the second-order AFM–PM transition.

Two anomalies are still present in the $M(T)$ dependences at 500 and 1000 Oe (figure 5).

Distinct peaks corresponding to the Curie and the Néel temperatures are no longer observed (compared with the low field measurements in figure 4). There are however two cusps (marked with arrows) on the $M(T)$ dependences, which can be associated with the phase transition locations. Moreover, the locations of the cusps depend on the magnetic field. The Néel temperature continues to shift to lower temperature but the Curie temperature shifts in the opposite direction with increasing magnetic field. As expected, the difference between ZFC and FC data is significantly reduced compared with 100 Oe.

Figure 6 shows the $M(T)$ behavior at 3.5 and 5 kOe.

The maxima at the transition points disappear and the magnetization exhibits a monotonic decrease with increasing temperature. As follows from the $\mathrm{d}M/\mathrm{d}T$ behavior (figure 6, inset), a single minimum is observed at every field, in good agreement with the heat capacity data (see below). It is noticeable that the transition temperature (taken as the minimum of $\mathrm{d}M/\mathrm{d}T$) shifts towards higher temperatures with increasing magnetic field. $\mathrm{d}M/\mathrm{d}T$ shows an asymmetric minimum at 3.5 kOe, but a nearly symmetric one at 5 kOe, which can be related to the disappearance of the AFM phase. As will be shown below (see the heat capacity data), the critical field value required to suppress the AFM ordering is 5 kOe. The temperature dependences of the real and imaginary components of ac magnetic susceptibility measured along the *b* axis from 5 to 300 K do not reveal additional phase transitions in Tb, and therefore they are not shown here for conciseness.

4. Magnetothermal properties

The temperature dependences of the heat capacity with the magnetic field applied along the easy magnetization *b* axis of

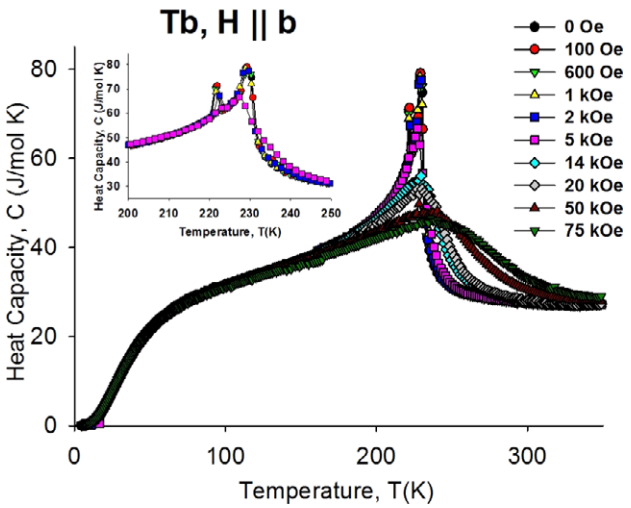

Figure 7. Temperature dependence of the heat capacity of Tb in several magnetic fields between 0 and 75 kOe applied along the *b* axis from 1.5 to 350 K. The inset shows temperature dependences of the heat capacity of Tb in low magnetic fields between 0 and 5 kOe applied along the *b* axis from 200 to 250 K.

Tb measured in the temperature interval from 1.5 to 350 K are shown in figure 7.

Two peaks corresponding to the Curie and the Néel temperatures are observed at ∼222 and 229 K, respectively, in zero magnetic field. The peak positions agree well with the results reported in the literature [18, 19]. The sharp peak at 222 K corresponding to the Curie temperature represents a minor anomaly compared with the broad λ-type maximum peaking at 229 K, corresponding to the Néel temperature. This behavior is consistent with the different natures of the two transitions: first order at the Curie temperature, and second order at the Néel temperature. The magnitude of the sharp peak at the Curie temperature is indicative of a small entropy change involved in this phase transition, and therefore it may be characterized as a weakly first-order phase transformation. In low magnetic fields (less than 5 kOe) the $C(T)$ curves exhibit two maxima (see the inset), but at 5 kOe the 222 K maximum disappears, indicating that the AFM–FM transition is suppressed by 5 kOe magnetic field. In high magnetic fields, the λ-shape peak at 229 K becomes a broad maximum that corresponds to a single FM–PM transition. Upon increasing the magnetic field, this broad maximum shifts slowly towards high temperatures, in agreement with the $M(T)$ data.

5. Discussion

Experimental data presented above generally agree with the previous results [13, 15, 17, 23]. The *H*–*T* phase diagram with the magnetic field applied along the easy magnetization (*b* crystallographic) direction constructed based on our data is shown in figures 8(a) and (b).

The helix AFM phase exists from ∼222 to 228 K in magnetic fields lower than ∼160 Oe. The overestimated critical field values of 300–800 Oe reported in the past are most likely the result of higher levels of impurities in the samples, which played the role of pinning sites, thus preventing the transformation of the helix AFM phase by increasing magnetic field. The $H_{crit}(T)$ dependence is a slightly asymmetrical bell-like function with the apparent maximum at 226 K. The critical field is zero at both the Curie and Néel temperatures, which indicates that the helical ordering is easily suppressed by even the smallest magnetic fields at these points.

With increasing field, a broad region of an intermediate phase is observed in the same temperature interval (i.e. between ∼221 and 228 K) in fields up to 5 kOe. According to the theoretical investigations [8] and elastic modulus [12] measurements made previously, we believe that this intermediate phase has a fan structure. Magnetic and magnetothermal properties measured in the present work do not contain any peculiar features which could be directly associated with the fan-like phase existence. However, the locations of the phase boundaries determined from the anomalies of the measured properties allowed us to determine the approximate region of

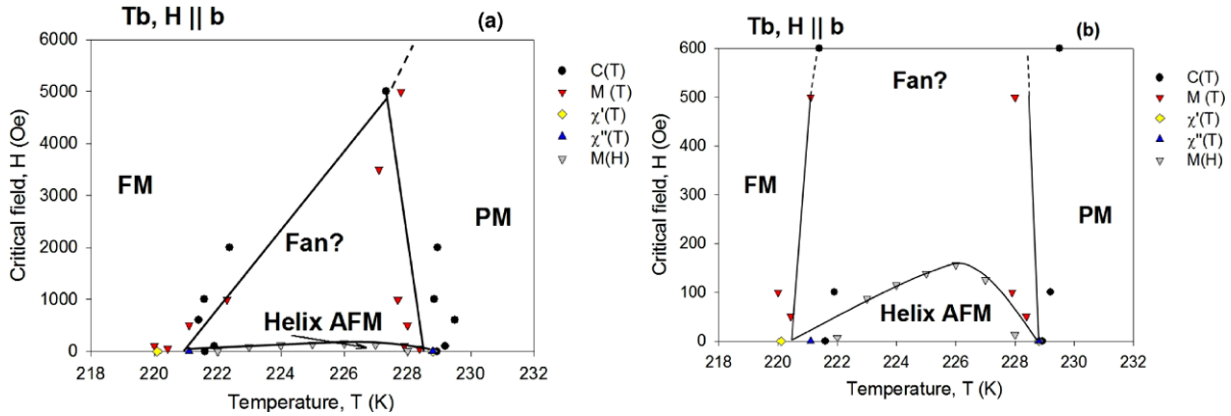

Figure 8. (a) The magnetic phase diagram of Tb in intermediate magnetic fields with the magnetic-field vector parallel to the easy magnetization direction (*b* axis) of the crystal at 218 to 234 K, and 0 to 6 kOe. (b) The magnetic phase diagram of Tb in low magnetic fields with the magnetic-field vector parallel to the easy magnetization direction (*b* axis) of the crystal from of 218 to 234 K, and 0 to 600 Oe.

this phase existence. The fan phase is located between the ferromagnetic and paramagnetic states, i.e. in the temperature range ∼221–229 K with the high field limit of 5 kOe. In the low field region (as described above), it is replaced by the helix AFM structure. The fan structure disappears at ∼227.3 K and ∼5 kOe. The main feature of the phase diagram presented here is the relatively broad region of the fan phase. In the previous studies, only one phase diagram containing the fan phase has been reported [17]; other reports did not include this phase in the diagrams. However, the question of whether this is a fan-like structure or a different distortion of a helix remains open.

In the magnetic fields exceeding 5 kOe, where only two phases (PM and FM) remain, the phase transition boundaries in Tb are rather difficult to determine from the heat capacity data, since the curves exhibit broad maxima. Since it is a second-order phase transition, the location of the PM–FM boundary should remain nearly constant in fields exceeding ∼5 kOe.

In the temperature range between the Curie temperature and the temperature where the fan phase vanishes, $\frac{dH_{crit}}{dT} > 0$ and the curve represents the phase boundary of a first-order FM–fan transition. From the other side, in the region where $\frac{dH_{crit}}{dT} < 0$, the curve $H_{crit}(T)$ is the phase boundary of the second-order fan–PM transition. The point where the phase boundary of the first order turns into the phase boundary of the second order is located at 227 K and ∼5 kOe. Thus according to Landau theory this point is the tricritical one, reflecting coexistence of FM, PM and fan phases.

6. Conclusion

Detailed heat capacity, magnetization and ac-susceptibility measurements of single crystal terbium in applied magnetic fields up to 75 kOe along *b* and *a* axes have been carried out from 4.2 to 350 K. This information, together with the known ferromagnetic state below 221 K and the PM state above 229 K, has allowed us to construct a magnetic phase diagram with the magnetic field applied in the basal plane (along the easy magnetization *b* direction) of single crystal Tb. The helical antiferromagnetic structure exists from 221 to 228 K. The maximum critical field of the helical ordering is ∼160 Oe, correcting the overestimated values of 300–800 Oe reported earlier. A magnetic phase, which we believe is of the fan type, has been located between 221 and 228 K in magnetic fields lower than 5 kOe. This critical field is about ten times higher when compared with theoretical predictions and previous experiments, which may be related to the higher purity of our crystals. Even though the presence of the fan-like phase has not been strictly confirmed, the thermodynamic conditions for its likely presence have been established, being compatible with previous elastic and magnetic experiments. However, neutron scattering experiments are required to firmly establish the fan structure. Hence, the phase relationships presented here are more representative of the intrinsic behaviors of Tb. A tricritical point is located at 227 K and ∼5 kOe.

Acknowledgments

Work at the Ames Laboratory is supported by the Office of Basic Energy Sciences, Materials Sciences and Engineering Division of the Office of Science of the US Department of Energy, under contract No DE-AC02-07CH11358 with Iowa State University (YaM, VKP and KAG). AMT and VIZ acknowledge support by the AMT&C Group, UK.

References

[1] Jensen J and Mackintosh A R 1991 *Rare Earth Magnetism: Structure and Excitations* (Oxford: Clarendon)
[2] Thoburn W C, Legvold S and Spedding F H 1958 *Phys. Rev.* **112** 56
[3] Hegland D E, Legvold S and Spedding F H 1963 *Phys. Rev.* **131** 158
[4] Koehler W C, Child H R, Wollan E O and Cable J W 1963 *J. Appl. Phys.* **34** 1335
[5] Chernyshov A S, Tsokol A O, Tishin A M, Gschneidner K A Jr and Pecharsky V K 2005 *Phys. Rev.* B **71** 184410
[6] Darnell F J 1963 *Phys. Rev.* **132** 1098
[7] Dietrich O W and Als-Nielsen J 1967 *Phys. Rev.* **162** 315
[8] Nagamiya T and Kitano Y 1964 *Prog. Theor. Phys. Japan* **31** 1
[9] Isci C and Palmer S B 1978 *J. Phys. F: Met. Phys.* **8** 247
[10] Herz R and Kronmueller H 1978 *J. Magn. Magn. Mater.* **9** 273
[11] Wilkinson M K, Koehler W C, Wollan E O and Cable J W 1961 *J. Appl. Phys.* **32** S48
[12] Jiles D C, Blackie G N and Palmer S B 1981 *J. Magn. Magn. Mater.* **24** 75
[13] Jiles D C, Palmer S B, Jones D W, Farrant S P and Gschneidner K A Jr 1984 *J. Phys. F: Met. Phys.* **14** 3061
[14] Bagguley D M S and Howe F A 1986 *J. Magn. Magn. Mater.* **58** 191
[15] Maekawa S, Treder R A, Tachiki M, Lee M C and Levy M 1976 *Phys. Rev.* B **13** 1284
[16] Andreenko A S, Belov K P, Nikitin S A and Tishin A M 1989 *Sov. Phys.—Usp.* **32** 649
[17] Kataev G I, Sattarov M R and Tishin A M 1989 *Phys. Status Solidi* a **114** K79
[18] Jennings L D, Stanton R M and Spedding F H 1957 *J. Chem. Phys.* **27** 909
[19] Lounasmaa O V and Sundstroem I J 1966 *Phys. Rev.* **150** 399
[20] Gschneidner K A Jr 1993 *J. Alloys Compounds* **193** 1
[21] Nikitin S A, Tishin A M and Bykhover S V 1989 *Phys. Status Solidi* a **114** K99
[22] Nikitin S A, Tishin A M, Bezdushnyi R V, Spichkin Yu I and Red'ko S V 1991 *J. Magn. Magn. Mater.* **92** 397
[23] Andrianov A V, Savel'eva O V, Bauer E and Paul Ch 2005 *Phys. Rev.* B **72** 132408
[24] Gschneidner K A Jr and Daane A H 1988 *Handbook on the Physics and Chemistry of Rare Earths* vol 11 ed K A Gschneidner Jr and L Eyring (Amsterdam: Elsevier)
[25] Chen D X, Pardo E and Sanchez A 2002 *IEEE Trans. Magn.* **38** 1742
[26] Pecharsky V K, Moorman J O and Gschneidner K A Jr 1997 *Rev. Sci. Instrum.* **68** 4196
[27] Oosthuizen C P and Alberts L 1975 *J. Magn. Magn. Mater.* **1** 76
[28] Greenough R R and Hettiarachchi N F 1983 *J. Magn. Magn. Mater.* **31–34** 178